

Geospatial mapping of health risk from trace metal(loid)s in the soil at an abandoned painting factory

Andrijana Miletić¹ , Aleksandra Savić² , Latinka Slavković-Beškoski² , Aleksandar Đorđević³ , Snežana Dragović⁴ , Ranko Dragović⁵ , Antonije Onjia¹ 

¹ Faculty of Technology and Metallurgy, University of Belgrade, Karnegijeva 4, 11120 Belgrade, Serbia

² Anahem Laboratory, Mocartova 10, 11160 Belgrade, Serbia

³ Faculty of Agriculture, University of Belgrade, Nemanjina 6, 11080 Belgrade, Serbia

⁴ Vinča Institute of Nuclear Sciences – National Institute of the Republic of Serbia, University of Belgrade, P.O. Box 522, Belgrade, Serbia

⁵ University of Niš, Faculty of Sciences and Mathematics, Department of Geography, Višegradska 33, 18000 Niš, Serbia

Keywords:

Heavy metals,
GIS,
ELCR,
Hazard quotient.

Abstract

A survey was made to analyze the geostatistical (GIS) distribution of the health risk of toxic trace metal(loid)s in the industrial soil located in the facility of an abandoned paints manufacturing company. A total of eighty surface soil samples were collected, and their concentrations determined. The mean concentration values of the elements were 7.8; 2.7; 55; 49; 0.21; 56; 114; and 239 mg/kg for As, Cd, Cr, Cu, Hg, Ni, Pb, and Zn, respectively. There was no non-carcinogenic health risk from the soil samples for adults, but it was hazardous soil for children with the excess lifetime cancer risk (ELCR) values exceeding the reference value of 10⁻⁴ for all studied samples. Most contributing toxic metal(loid)s to non-carcinogenic risk were Cr and As, whereas Pb and As were most responsible for cancer risk. Geospatial mapping of the hazard index (HI) and ELCR localized different hotspots seriously polluted by toxic metal(loid)s, which pose a significant risk in the area. These hotspots coincided with the evidence of transport-related activities and spillage of chemicals in the past. This GIS spatial distribution study could be a valuable aid in remediation planning.

1. Introduction

Rapid technological development has caused a ceasing of the operation of a large number of manufacturing companies. Many of these companies have been located in an urban area, so their land could be used for other purposes, such as housing, parks, commerce, etc. Anyhow, soil quality should be investigated to figure out whether pollution from former industrial activities has taken place (Wcisło et al., 2002).

Numerous studies have dealt with multivariate analysis of toxic trace metal(loid)s pollution of soil using principal component and hierarchical cluster analyses (PCA, HCA) (Slavković et al., 2004; Dragović et al., 2013; Dragović et al., 2018; Onjia, 2016; Škrbić et al., 2018; Tanić et al., 2018; Egbueri et

al., 2020). These studies were aimed to recognize the soil contamination pattern and pinpoint the potential pollution sources. Also, ecological risk indices have been commonly evaluated to get a better insight into soil pollution (Dragović et al., 2014; Çulha, et al., 2017; Relić et al., 2019; Radomirović et al., 2020; Lukić et al., 2020; Minkina et al., 2020).

On the other hand, the essential part of the soil contamination investigation is to estimate the potential health risk originated from toxic trace metal(loid)s in the soil (Loredo et al., 2003; Gržetić and Ghariani, 2008). Health risk assessment (HRA), as a process used to estimate health effects of toxic trace metal(loid)s humans residing around the abandoned factory, should be carried out (EPA, 2013). HRA consist of four necessary steps: identification of hazard, exposure as-

assessment, dose-response assessment, and risk characterization (EPA, 2013). Hazard identification, as the first step, aims to analyze toxic elements present at a given location, including their soil contents and spatial distribution. The second step, i.e. exposure assessment, determines the frequency, duration, and intensity of human exposures to a toxic element. This is usually carried out by estimating the chronic daily intake (CDI) value for specific toxic element through ingestion, inhalation and dermal contact routes by children and adults. Children and adults are different in terms of both mental and physiological aspects (EPA, 2011). Dose-response assessment uses the reference dose (RfD) and cancer slope factor (CSF) to evaluate the non-carcinogenic and carcinogenic toxicity due to exposure to a toxic element, respectively. The last step comprising the risk characterization integrates all previously gathered data to quantify risks (EPA, 2011). The non-carcinogenic health risk may be assessed using the risk quotient (RQ) for each element and sample. In parallel, the excess lifetime cancer risk (ELCR) parameter is used to estimate carcinogenic risk.

Having in mind that the potential health risk of the soil pollution may be non-uniformly distributed over the study area, a geostatistical evaluation (Petrović et al., 2018; Trujillo-González et al., 2019) is needed. A spatial mapping using a geostatistical information system (GIS) enables meaningful information about soil pollution and the economic cost in soil sampling and analysis since excessive sampling and testing are not necessary. The GIS kriging interpolation method may successfully describe and predict the spatial distribution of toxic trace metal(loid)s concentrations of a non-sampled area.

This study deals with the trace elements contamination of the soil in the facility of an abandoned painting factory (Duga doo, Belgrade). The pollution by toxic trace metal(loid)s of this area has been studied recently (Radomirović et al., 2020), but no health risk assessment was made. The aim of this study is to identify pollution hotspots and to identify anthropogenic sources of the toxic meta(loid)s contamination of soil by geospatial mapping of HRA results.

2. Materials and methods

2.1. Study area, sample handling and preparation

The study area of approximately 11 ha is located in the Duga a.d. facility in Belgrade (Serbia). A total of 80 composite samples of surface soil were taken in duplicate. The distribution of the sampling points is shown in Figure 1. A soil core sampler was used for sampling. A composite sample consisting

of 5 individual samples was transferred into a plastic jar and kept cool until analysis. The samples were air-dried in the laboratory, pulverized, and sieved (2 mm pores). Afterwards, the samples were subjected to microwave-assisted digestion as described elsewhere (Radomirović et al., 2020).

2.2. Instrumental measurement and QA/QC control



Figure 1. The study area and distribution of sampling sites.

A concentrated mixture of HNO₃, HCl, and H₂O₂ was used for pseudo-total metal(loid)s digestion. The obtained solution with the dissolved metal(loid)s were analyzed by an Atomic Absorption Spectrometry (AAS) using a Perkin-Elmer model Analyst 100 instrument, which is equipped with a deuterium background correction lamp and hollow-cathode/electrodeless discharge lamps. Apart from the measurements of the concentrations of Cr, Cd, Pb, Ni, Zn, Cu, the concentration of As and Hg were determined using a model MHS-15 cold vapour accessory (Perkin-Elmer).

Quality assurance and quality control (QA/QC) was done by analyzing blanks and duplicates, as well as a NIST Certified Reference Material SRM 2711a (Montana II Soil). All recoveries obtained were between 83-104%, and the relative standard deviation was within 12%.

2.3. Health risk assessment

CDI for the different potential exposure routes for toxic metal(loid)s in soil may be estimated using the following Equations (EPA, 2013)

$$CDI_{ingest} = (C \cdot IngR \cdot EF \cdot ED \cdot CF) / (BW \cdot AT) \quad (1)$$

$$CDI_{inhal} = (C \cdot InhR \cdot EF \cdot ED \cdot CF) / (PEF \cdot BW \cdot AT) \quad (2)$$

$$CDI_{dermal} = (C \cdot SA \cdot SL \cdot ABF \cdot EF \cdot ED \cdot CF) / (BW \cdot AT) \quad (3)$$

Table 1. HRA exposure parameters for the ingestion, inhalation and dermal contact exposure pathways (EPA 2013).

Parameter	Unit	Adults	Children
Concentration of heavy metal (C)	mg/kg		
Ingestion rate (IngR)	mg/d	100	200
Exposure frequency (EF)	d/year	350	350
Exposure duration (ED)	years	24	6
Bodyweight (BW)	kg	70	15
Average time (AT)	days	8760	2190
Inhalation rate (InhR)	m ³ /d	15	10
Particulate emission factor (PEF)	m ³ /kg	1.36·10 ⁹	1.36·10 ⁹
Skin surface area (SA)	cm ²	5700	2800
Soil adherence factor (SL)	mg/cm ²	0.07	0.2
Dermal absorption factor (ABF)	none	0.01	0.001
Conversion factor (CF)	kg/mg	10 ⁻⁶	10 ⁻⁶

where the meanings and values of the exposure parameters in Eqs. (1) - (3) were given in Table 1.

Hazard quotient (HQ) characterizes non-carcinogenic risk. It is a unitless number calculated as the ratio of CDI and RfD of an individual toxic element (Eq. 4)

$$HQ = CDI/RfD \tag{4}$$

Hazard Index (HI) represents the summation of all individual HQs (Eq. 5)

$$HI = HQ_{ingest} + HQ_{inhal} + HQ_{dermal} \tag{5}$$

where HQ_{ingest} , HQ_{inhal} , and HQ_{dermal} are risks contributions through ingestion, inhalation and dermal contact routes.

Carcinogenic risk estimated as excess lifetime cancer risk (ELCR) is defined as the probability of an individual to develop cancer over a lifetime due to exposure to potential carcinogens. The mathematical representation of this parameter is given in Eq. (6).

Table 2. RfD (mg/kg-day) and CSF ((mg/kg-day)⁻¹) for the different toxic metal(loid)s and expose pathways.

	RfD _{ingest}	RfD _{inhal}	RfD _{dermal}	CSF _{ingest}	CSF _{inhal}	CSF _{dermal}
As	3.00E-04	1.23E-04	1.23E-04	1.50E+00	4.30E-03	3.66E+00
Cd	1.00E-03	1.00E-05	1.00E-05	-	6.30E+00	-
Cr	3.00E-03	2.86E-05	6.00E-05	5.00E-01	4.20E+01	2.00E+01
Cu	4.00E-02	4.02E-03	1.20E-02	-	-	-
Hg	3.00E-04	8.57E-05	2.10E-05	-	-	-
Ni	2.00E-02	2.06E-02	5.40E-03	-	-	-
Pb	3.50E-03	3.52E-03	5.25E-04	8.50E-03	4.20E-02	-
Zn	3.00E-01	3.00E-01	6.00E-02	-	-	-

$$ELCR = CDI \cdot CSF \tag{6}$$

The total ELCR is a unitless probability calculated from the contribution of each carcinogenic substance for all expose routes according to the following equation:

$$ELCR = ELCR_{ingest} + ELCR_{inhal} + ELCR_{dermal} \tag{7}$$

The health risks of toxic metal(loid)s in the soil are estimated using CSF and RfD values (EPA, 2011), as shown in Table 2.

2.4. Geostatistical data analysis

GIS maps of the trace metal(loid)s in the soil were created using Surfer software (Golden Software Inc.). Due to the number of buildings and infrastructure installations, the sampling points were unevenly distributed. Hence, ordinary kriging was used to develop the GIS spatial interpolation maps of health risks in the area.

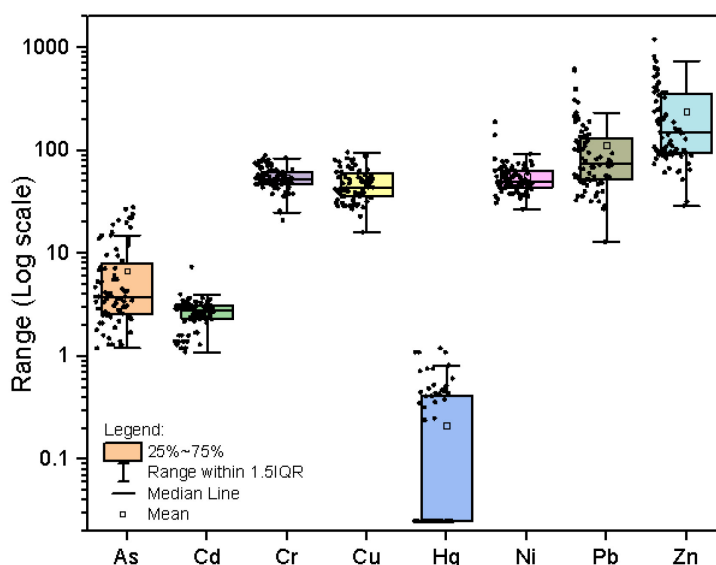


Figure 2. Trace metal(loid)s distribution in the soil (mg/kg).

3. Results and discussion

3.1. Trace metal(loid)s distribution

Figure 2 depicts the distribution of the eight trace metal(loid)s in the studied soil from an abandoned painting manufacturing site. The results indicate that the concentrations of the studied metal(loid)s varied significantly and decreased in the following order: Zn > Pb > Ni > Cr > Cu > As > Cd > Hg. The average concentration values (mg/kg) are as follows: As (7.8); Cd (2.7); Cr (55); Cu (49); Hg (0.21); Ni (56); Pb (114); and Zn (239). These average metal(loid)s concentrations exceeded the target limits (mg/kg) for Ni (35), Cu (36), Cd (0.8) and Pb (85) (Official Gazette of the Republic of Serbia, 2018).

3.2. Health risk assessment

3.2.1. Non-carcinogenic risk

Table 3 presents non-carcinogenic risks estimated based on CDI and RfD values for ingestion, inhalation and dermal contact pathways, presented in terms of HQs AND HIs for children and adults.

There will be no obvious non-carcinogenic human health risk when HQ and HI values are ≤ 1 . However, there are some samples in which the concentrations of As, and Pb in particular, are very high. Consequently, HQ and HI for these samples exceed the limit value of one for children. The risk of Pb in polluted soil area for children is due to the oral intake

route. No individual non-carcinogenic human health risk was estimated in the area for adults. These risk assessment results show that the most significant concern for both populations is mainly attributed to Pb. The total minimum, mean, and maximum HI values were 0.08; 0.19; 0.47; and 0.38; 1.10; 2.92; for adults and children, respectively. The total HI for children greater the one scenario was found in 45 % of the analyzed soil samples. The oral ingestion route is a major contributor to the total non-carcinogenic health risk.

3.2.2. Carcinogenic risk

The carcinogenic HRA was based on the following metal(loid)s: As; Cd; Cr; and Pb. Acceptable cancer risk is in the range of 10^{-6} to 10^{-4} (EPA, 2013). The individual and total Σ ELCR for children and adults are estimated from the contribution of each carcinogenic metal(loid)s in the soil for all the expose routes using Eqs. (6) and (7). The results of the individual ELCR values are given in Table 4. The individual ELCR was found to be in the range of $4.3 \cdot 10^{-5}$ to $2.1 \cdot 10^{-4}$ and $2.0 \cdot 10^{-4}$ to $1.1 \cdot 10^{-3}$ for adults and children, respectively. The ELCR values are mostly influenced by the ingestion pathway. In general, children are more at risk than adults due to the presence of toxic metal(loid)s this study area. The total Σ ELCR results ranged from $4.3 \cdot 10^{-5}$ to $1.2 \cdot 10^{-4}$ and $2.0 \cdot 10^{-4}$ to $1.1 \cdot 10^{-3}$ for adults and children, respectively. Additionally, 70 % and 100 % of the total Σ ELCR results for adults and children, respectively, exceed the threshold value for cancer risk of 10^{-4} . It

Table 3. HQs and HIs for the ingestion, inhalation and dermal contact pathways for (a) adults and (c) children.

HQ or HI	As	Cd	Cr	Cu	Hg	Ni	Pb	Zn
HQ _{a,ing} mean	0.0310	0.0037	0.0252	0.0017	0.0010	0.0038	0.0446	0.0011
HQ _{a,ing} max	0.1279	0.0101	0.0406	0.0033	0.0055	0.0129	0.2411	0.0055
HQ _{a,ing} min	0.0055	0.0015	0.0096	0.0005	0.0001	0.0018	0.0051	0.0001
HQ _{a,inh} mean	0.0000	0.0000	0.0000	0.0000	0.0000	0.0000	0.0000	0.0000
HQ _{a,inh} max	0.0000	0.0000	0.0000	0.0000	0.0000	0.0000	0.0000	0.0000
HQ _{a,inh} min	0.0000	0.0000	0.0000	0.0000	0.0000	0.0000	0.0000	0.0000
HQ _{a,derm} mean	0.0030	0.0147	0.0503	0.0002	0.0006	0.0006	0.0119	0.0002
HQ _{a,derm} max	0.0124	0.0404	0.0811	0.0004	0.0031	0.0019	0.0641	0.0011
HQ _{a,derm} min	0.0005	0.0060	0.0191	0.0001	0.0001	0.0003	0.0014	0.0000
HI _{a,mean}	0.0340	0.0184	0.0755	0.0019	0.0015	0.0044	0.0564	0.0013
HI _{a,max}	0.1403	0.0506	0.1217	0.0037	0.0086	0.0149	0.3052	0.0066
HI _{a,min}	0.0060	0.0075	0.0287	0.0006	0.0002	0.0021	0.0064	0.0002
HQ _{c,ing} mean	0.2895	0.0344	0.2353	0.0157	0.0090	0.0358	0.4158	0.0102
HQ _{c,ing} max	1.1933	0.0946	0.3793	0.0307	0.0511	0.1208	2.2502	0.0511
HQ _{c,ing} min	0.0511	0.0141	0.0895	0.0051	0.0011	0.0173	0.0475	0.0012
HQ _{c,inh} mean	0.0000	0.0000	0.0000	0.0000	0.0000	0.0000	0.0000	0.0000
HQ _{c,inh} max	0.0000	0.0000	0.0000	0.0000	0.0000	0.0000	0.0000	0.0000
HQ _{c,inh} min	0.0000	0.0000	0.0000	0.0000	0.0000	0.0000	0.0000	0.0000
HQ _{c,derm} mean	0.0020	0.0096	0.0329	0.0001	0.0004	0.0004	0.0078	0.0001
HQ _{c,derm} max	0.0081	0.0265	0.0531	0.0003	0.0020	0.0013	0.0420	0.0007
HQ _{c,derm} min	0.0003	0.0039	0.0125	0.0000	0.0000	0.0002	0.0009	0.0000
HI _{c,mean}	0.2915	0.0441	0.2682	0.0158	0.0094	0.0362	0.4236	0.0103
HI _{c,max}	1.2015	0.1211	0.4324	0.0310	0.0532	0.1221	2.2922	0.0518
HI _{c,min}	0.0515	0.0180	0.1020	0.0052	0.0011	0.0174	0.0484	0.0013

Table 4. ELCR for the ingestion, inhalation and dermal contact pathways for adults and children

ELCR	As	Cd	Cr	Pb
ELCR _{a,ing} mean	1.40E-05	0.00E+00	3.78E-05	1.33E-06
ELCR _{a,ing} max	5.75E-05	0.00E+00	6.10E-05	7.17E-06
ELCR _{a,ing} min	2.47E-06	0.00E+00	1.44E-05	1.51E-07
ELCR _{a,inh} mean	4.41E-18	2.56E-15	3.50E-13	7.22E-16
ELCR _{a,inh} max	1.82E-17	7.04E-15	5.65E-13	3.91E-15
ELCR _{a,inh} min	7.80E-19	1.05E-15	1.33E-13	8.25E-17
ELCR _{a,derm} mean	1.36E-06	0.00E+00	6.03E-05	0.00E+00
ELCR _{a,derm} max	5.60E-06	0.00E+00	9.73E-05	0.00E+00
ELCR _{a,derm} min	2.40E-07	0.00E+00	2.30E-05	0.00E+00
ΣELCR _a mean	1.53E-05	2.56E-15	9.82E-05	1.33E-06
ΣELCR _a max	6.31E-05	7.04E-15	1.58E-04	7.17E-06
ΣELCR _a min	2.71E-06	1.05E-15	3.73E-05	1.51E-07
ELCR _{c,ing} mean	1.30E-04	0.00E+00	3.53E-04	1.24E-05
ELCR _{c,ing} max	5.37E-04	0.00E+00	5.69E-04	6.69E-05
ELCR _{c,ing} min	2.30E-05	0.00E+00	1.34E-04	1.41E-06
ELCR _{c,inh} mean	1.37E-17	7.98E-15	1.09E-12	2.25E-15
ELCR _{c,inh} max	5.66E-17	2.19E-14	1.76E-12	1.22E-14
ELCR _{c,inh} min	2.43E-18	3.26E-15	4.15E-13	2.57E-16
ELCR _{c,derm} mean	8.90E-07	0.00E+00	3.95E-05	0.00E+00
ELCR _{c,derm} max	3.67E-06	0.00E+00	6.37E-05	0.00E+00
ELCR _{c,derm} min	1.57E-07	0.00E+00	1.50E-05	0.00E+00
ΣELCR _c mean	1.31E-04	7.98E-15	3.92E-04	1.24E-05
ΣELCR _c max	5.41E-04	2.19E-14	6.33E-04	6.69E-05
ΣELCR _c min	2.32E-05	3.26E-15	1.49E-04	1.41E-06

means the studied area should be avoided before the remediation measures are undertaken.

3.3. Geostatistical mapping

The geospatial mapping of toxic trace metal(loid)s in soil was made using a GIS approach. Firstly, the element concentrations were interpolated with the ordinary kriging technique. Then, the GIS-based maps of non-carcinogenic and carcinogenic risk indices were compared. The obtained GIS maps are presented in Figure 3. In general, the darker red colour area in the filled contour maps indicate the highest risk, while the green coloured area suggested low risks. A few red hotspots of high HIs and ELCRs were identified in Figure 3. A quite different distribution of hotspots for non-carcinogenic and carcinogenic risks was obtained.

These maps of HIs show no exceedance of a level of one for adults in the study area and reveal the sub-area with unacceptable high risk for children ($HI > 1$). The ELCR results locate the highest risk at the one hotspot for adults and several hotspots for children. These hotspots were located in a different part of the area. Moreover, the geospatial pattern reveals the sub-area with severe HI and ELCR hotspots for children. Lead, followed by As, are the most responsible metal(loid)s for non-carcinogenic risk. On the other hand, ELCR results indicate Cr and As as the most detrimental metal(loid)s that pose the cancer risk in the area.

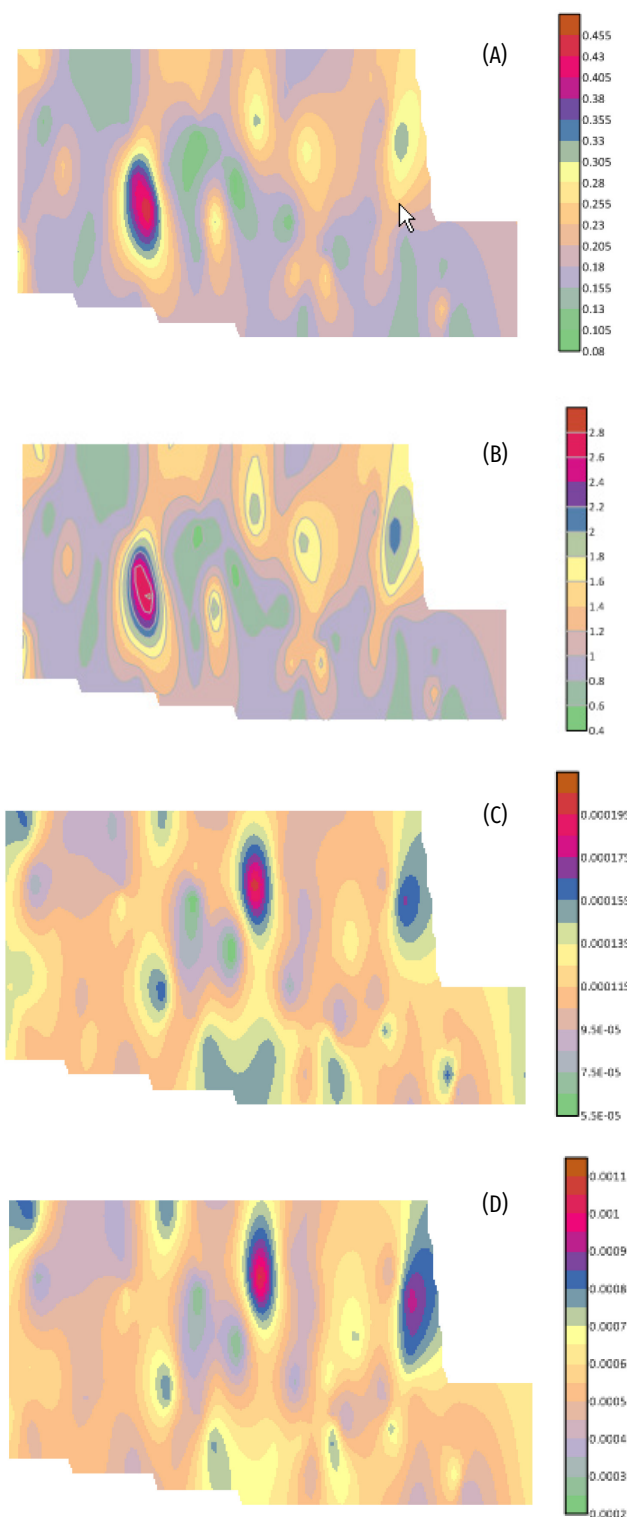


Figure 3. Geospatial distribution maps of HI and ELCR in the soil. (A) HI_a; (B) HI_c; (C) ΣELCR_a; (D) ΣELCR_c.

A reasonable association was readily displayed between these hotspots and risks with the former industrial activities. The hotspot with the highest HI values was located in the area of the abandoned car mechanic workshop, where vehicle-related activities had been concentrated. The main

ELCR hotspot is placed in the previous chemical waste storage area. The second ELCR hotspot coincided with the area used for the manipulation with the raw materials in the past. These findings were harmonized with the previous investigation of the same location (Radomirović *et al.*, 2020)

In this work, it seems reasonable to conclude that Pb, Cr and As constitute an anthropogenic component of the soil contamination, which is associated with specific activities in the past. Apart from this, the other toxic metal(loid)s appear to originate from the soil parent materials that are mostly the alluvial river deposits from the Danube River bank terrace (Mihailović *et al.*, 2015).

4. Conclusion

The results obtained in the analysis of soil from an abandoned painting manufacturing site show that the eight studied toxic trace metal(loid)s varied significantly and decreased in the following order: Zn > Pb > Ni > Cr > Cu > As > Cd > Hg. The average metal(loid)s concentrations in soil showed higher than target limits for Ni, Cu, Cd and Pb.


Geospatial mapping of health risk due to toxic trace metal(loid)s content in soil indicated similar spatial distribution patterns for adults and children. However, the spatial pattern between carcinogenic and non-carcinogenic risk differs significantly. Moreover, children are more vulnerable to the carcinogenic and non-carcinogenic risks, with 45 % of the studied soil samples exceeded reference value one of hazard index and 100 % of the total ΣELCR values exceeded the cancer threshold risk of 10^{-4} . It means that children should avoid this area before the remediation measures are undertaken. The primary pathway to exposure to cancer and non-cancer risks is ingestion.

In conclusion, GIS mapping of HRA results may effectively identify hotspots and indicate anthropogenic sources of the toxic metal(loid)s contamination of soil. These findings may help in the subsequent remediation of the polluted soil.

Acknowledgement

This work was supported by the Ministry of Education, Science and Technological Development of the Republic of Serbia (Contract No. 451-03-68/2020-14/200135).

ORCID iDs

Andrijana Miletić  <https://orcid.org/0000-0002-6310-5235>
 Aleksandra Savić  <https://orcid.org/0000-0002-1210-5497>
 Latinka Slavković Beškoski  <https://orcid.org/0000-0002-8650-5020>
 Aleksandar Đorđević  <https://orcid.org/0000-0002-2989-6483>
 Snežana Dragović  <https://orcid.org/0000-0003-0566-0182>
 Ranko Dragović  <https://orcid.org/0000-0002-4662-7808>
 Antonije Onjia  <https://orcid.org/0000-0002-5694-7960>

References

- Çulha, S.T., Çulha, M., Karayücel, İ., Çelik, M.Y., İşler, Y., 2017. Heavy metals in *Mytilus galloprovincialis*, suspended particulate matter and sediment from offshore submerged longline system, Black Sea. *International Journal of Environmental Science and Technology*, 14(2), 385-396.
- Dragović, S., Kovačević, M., Bajat, B., Onjia, A., 2018. Support vector machines for classification of soils according to geographic origin based on their radionuclide content. *Serbian Journal of Geosciences*, 4(1), 15-26.
- Dragović, R., Gajić, B., Dragović, S., Đorđević, M., Đorđević, M., Mihailović, N., Onjia, A., 2014. Assessment of the impact of geographical factors on the spatial distribution of heavy metals in soils around the steel production facility in Smederevo (Serbia). *J. Clean. Prod.* 84, 550-562.
- Dragović, S., Čujić, M., Slavković-Beškoski, L., Gajić, B., Bajat, B., Kilibarda, M., Onjia, A., 2013. Trace element distribution in surface soils from a coal burning power production area: A case study from the largest power plant site in Serbia. *Catena* 104, 288-296.
- Gržetić, I., Ghariani, R.H.A., 2008. Potential health risk assessment for soil heavy metal contamination in the central zone of Belgrade (Serbia). *J. Serb. Chem. Soc.* 73(8-9), 923-934.
- Egbueri, J.C., Ukah, B.U., Ubido, O.E., Unigwe, C.O., 2020. A chemometric approach to source apportionment, ecological and health risk assessment of heavy metals in industrial soils from southwestern Nigeria. *Int. J. Environ. Anal. Chem.* 1-19.
- EPA, 2002. Supplemental Guidance for Developing Soil Screening Levels for Superfund Sites. Office of Solid Waste and Emergency Response. DCOSWER 9355.4-24. US EPA, Washington.
- EPA, 2011. Exposure Factors Handbook (EFH), US EPA, Washington.
- EPA, 2013. Regional Screening Levels (RSLs), Risk Assessment, US EPA. Washington.
- Loredo, J., Ordonez, A., Charlesworth, S., De-Miguel, E., 2003. Influence of industry on the geochemical urban environment of Mieres (Spain) and associated health risk. *Environ. Geochem. Health* 25(3), 307-323.
- Lukić, J., Đurkić, T., Jovanović, L., Aleksić, G., Onjia, A., 2020. Total petroleum hydrocarbons distribution and health risk assessment of soil in the Niš railway junction. *Ecologica* 27(100), 597-604.

- Mihailović, A., Budinski-Petković, L., Popov, S., Ninkov, J., Vasin, J., Ralević, N. M., Vučinić Vasić, M., 2015. Spatial distribution of metals in urban soil of Novi Sad, Serbia, GIS based approach. *J. Geochem. Explor.* 150, 104–114.
- Minkina, T., Konstantinova, E., Bauer, T., Mandzhieva, S., Sushkova, S., Chaplygin, V., Burachevskaya, M., Nazarenko, O., Kizilkaya, R., Gülser, C., Maksimov, A., 2020. Environmental and human health risk assessment of potentially toxic elements in soils around the largest coal-fired power station in Southern Russia. *Environmental Geochemistry and Health*, 1-16.
- Official Gazette of the Republic of Serbia, 2018. Rulebook on limit values of pollutants, harmful and hazardous substances in soil, No. 30/2018.
- Onjia, A., 2016. Chemometric approach to the experiment optimization and data evaluation in analytical chemistry. University of Belgrade, Faculty of Technology and Metallurgy, Belgrade.
- Petrović, J., Dragović, R., Gajić, B., Đorđević, M., Dragović, S., 2018. Depth distribution of ¹³⁷Cs in soils from special nature reserve Banat sands, Serbia and assessment of doses to non-human biota. *Serbian Journal of Geosciences* 4(1), 1-14.
- Radomirović, M., Ćirović, Ž., Maksin, D., Bakić, T., Lukić, J., Stanković, S., Onjia, A., 2020. Ecological Risk Assessment of Heavy Metals in the Soil at a Former Painting Industry Facility. *Front. Environ. Sci.* 8, 560415.
- Relić, D., Sakan, S., Andelković, I., Popović, A., Đorđević, D., 2019. Pollution and health risk assessments of potentially toxic elements in soil and sediment samples in a petrochemical industry and surrounding area. *Molecules* 24, 2139.
- Škrbić, B., Buljovčić, M., Jovanović, G., Antić, I., 2018. Seasonal, spatial variations and risk assessment of heavy elements in street dust from Novi Sad, Serbia. *Chemosphere* 205, 452-462.
- Slavković, L., Škrbić, B., Miljević, N., Onjia, A., 2004. Principal component analysis of trace elements in industrial soils. *Environ. Chem. Lett.* 2(2), 105-108.
- Tanić, M., Onjia, A., Janković Mandić, L., Ćujić, M., Dinić, D., Dragović, S., 2018. Human health risk assessment due to natural radionuclides in soil affected by coal combustion: A case study from the surroundings of the largest thermoelectric power plant in Serbia. *Ecologica* 25, 5-11.
- Trujillo-González, J. M., Torres-Mora, M. A., Jiménez-Ballesta, R., Zhang, J., 2019. Land-use-dependent spatial variation and exposure risk of heavy metals in road-deposited sediment in Villavicencio, Colombia. *Environmental geochemistry and health* 41(2), 667-679.
- Wcisło, E., Ioven, D., Kucharski, R., Szdzuj, J., 2002. Human health risk assessment case study: an abandoned metal smelter site in Poland. *Chemosphere* 47(5), 507-515.